JOURNAL OF PROPULSION AND POWER
Vol. 9, No. 5, Sept.-Oct. 1993

High-Pressure Hypervelocity Electrothermal Wind-Tunnel Performance Study and Subscale Tests

Oussama F. Rizkalla* and Wallace Chinitz†
General Applied Science Laboratories, Ronkonkoma, New York 11779
F. Douglas Witherspoon‡
GT-Devices, Inc., Alexandria, Virginia 22312
and
Rodney L. Burton§
University of Illinois, Urbana, Illinois 61801

This article describes the results of a study to demonstrate the feasibility of a Mach 10 to 20 air breathing propulsion test facility. The key element of this wind tunnel is a heater which uses a continuous high-power electric arc discharge potentially capable of heating air to temperatures over 10,000 K and to pressures of 15,000 atm. The heated air is then expanded through a supersonic nozzle to obtain the test condition. The features unique to this facility are the heater design, which allows arbitrarily high pressures to be generated (limited only by the material strength of the chamber), and the use of liquid air which improves the heater efficiency and alleviates the problems associated with conventional arc heaters operating at high pressure. Analytical and experimental studies were conducted to determine the simulation limits of the facility and demonstrate stable operation of the heater with a cryogenic liquid, respectively. The analytical study indicated that the high pressure improves recombination chemistry in the facility nozzle by allowing chemical equilibrium to prevail to the freezing point. However, the high pressure also enhances the formation of nitric oxide which contaminates the test gas at roughly 5% by volume throughout the simulation envelope. The practical simulation limit of the facility was found to extend to about Mach 16, where pressure containment, high nozzle throat heat flux rates, and chemical freezing in the nozzle become limiting factors. The experimental study on a subscale, 2-ms test facility were successful in that steady arc discharges were observed with liquid nitrogen flowing into the arc chamber. The measured steady pressure in the arc chamber was 4559 psi, which is at least 20% greater than the maximum total pressure obtainable in conventional arc heaters.

Nomenclature

H = enthalpy
M = Mach number
$\dot{m}$ = mass flow
P = pressure
q = heat flux
Re = Reynolds number
s = specific entropy
T = temperature
t = time
V = velocity
η_n = nozzle performance parameter
θ = nozzle half-angle, deg

Subscripts
l = local quantity
t = reservoir quantity
w = property at a surface
∞ = freestream quantity

Introduction

A RENEWED international interest in hypersonic flight has generated a need for ground testing air breathing propulsion systems at simulated flight conditions above Mach 10.[1-5] In order to flight-qualify a propulsion system and relate ground test data to flight, true simulation of the relevant characteristics of air is required. Proper simulation of the flow physics and chemistry at hypervelocity conditions requires duplication of the local temperature, density, velocity, gas composition, and scale. The latter implies that the model engine must be appropriately sized (preferably to full scale) to closely simulate the residence time of the gas in the engine, and particularly in the combustor, where the time required to mix and react the fuel and oxidizer is of the order of the residence time. In addition, the facility test time must be sufficient to test critical engine systems and structures, to allow establishment of viscous-dominated phenomena such as separated flow regions, and to simulate nonadiabatic and catalytic wall effects. Although the total enthalpy requirement for hypervelocity simulation can be met, all facilities currently in operation are limited in one or more of the above test requirements because they cannot produce the requisite total pressure levels for sufficient duration, and/or cannot duplicate the conditions and the composition of air as they exist in flight.

The relative total pressure capabilities of various test facility concepts are summarized in Fig. 1. This figure shows the total pressure required for a typical National AeroSpace Plane (NASP) trajectory (1000 psf) as a function of flight Mach number for the freestream and for typical inlet and combustor entrance conditions. The total pressure varies exponentially with flight Mach number, and freestream total pressure quickly exceeds 1000 atm above about Mach 10. However, combustion and arc heaters are typically limited in total pressure to about 250 atm due to high plenum heat transfer rates and to arc stability and electrode burnout, respectively. This restricts simulation to between Mach 7 freestream (f.s.) and Mach

Presented as Paper 92-0329 at the AIAA 30th Aerospace Sciences Meeting and Exhibit, Reno, NV, Jan. 6–9, 1992; received March 2, 1992; revision received March 15, 1993; accepted for publication April 2, 1993. Copyright © 1993 by the American Institute of Aeronautics and Astronautics, Inc. All rights reserved.

*Scientist. Member AIAA.
†Principal Scientist; also Professor of Mechanical Engineering, Cooper Union, Nerken School of Engineering. Associate Fellow AIAA.
‡Scientist. Member AIAA.
§Associate Professor of Aeronautical Engineering; also Consultant to GT-Devices. Associate Fellow AIAA.

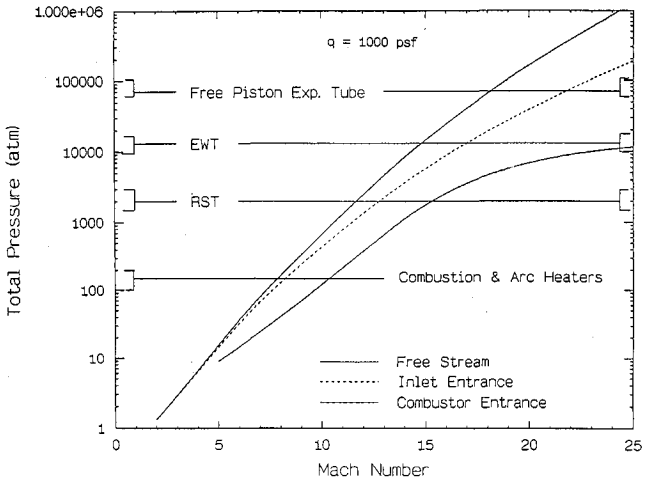

Fig. 1 Total pressure simulation capability of various facility concepts.

11–12 combustor inlet (c.i.). Reflected shock tunnels (RST) typically generate about 2000–3000 atm (Mach 12 f.s. to Mach 15 c.i.) due to structural limitations of the driver tube. However, test times are of the order of milliseconds. A free-piston-driven expansion tube, which adds kinetic energy by way of an unsteady expansion wave, can theoretically duplicate conditions which correspond to total pressures of 70,000–100,000 atm (Mach 18 f.s. to >Mach 25 c.i.), but does so at the expense of test time and model size.

The objective of the present research was to demonstrate, analytically and experimentally, the feasibility of building a high total pressure and enthalpy, air breathing propulsion test facility. The electrothermal wind tunnel (EWT) was initially conceptualized to produce mass flows up to 17 kg/s (37 lbm/s) for test times from 0.1 to 10 s at simulated Mach 20 test conditions. The corresponding nozzle exit area for a free-jet test (i.e., simulated inlet entrance conditions) is 2 ft^2. Figure 1 shows that the EWT is theoretically capable of obtaining total pressures between 10,000–20,000 atm (Mach 15 f.s. to Mach 25 c.i., depending on the limits of pressure containment).

The key element of the EWT is a heater which uses a continuous high-power arc discharge to ultimately heat cryogenic liquid air to high temperature and pressure. This concept is an extension of existing electrothermal plasma jet technology developed for electrothermal guns[6] and space thrusters.[7] The working fluid in these applications is either a gas or the ablated walls of the arc chamber. Here, the vaporized liquid air which is initially confined to a small diameter tube (referred to herein as the capillary), is mixed with more fluid to obtain the desired reservoir conditions. The gas is then expanded through a supersonic nozzle to produce the test conditions. A schematic diagram illustrating the facility concept is shown in Fig. 2, and the free-jet and direct-connect (combustor entrance) test conditions for the selected facility design points are listed in the Appendix.

The electrothermal heater is similar in principle to conventional arc heaters, but differs in several significant respects. First, the small diameter capillary allows arbitrarily high pressures to be generated, limited only by the material strength of the chamber walls. High pressure is required not only to duplicate the static pressures encountered in flight, but to more closely simulate the test gas composition. In essence, the dissociation of air at high capillary and reservoir temperatures is reduced and the chemistry during the nozzle expansion remains in equilibrium longer. Secondly, a liquid's high density and optically thick qualities reduce electrode and insulator burnout because more of the radiation emitted by the arc is absorbed by the liquid. This in turn results in an energy

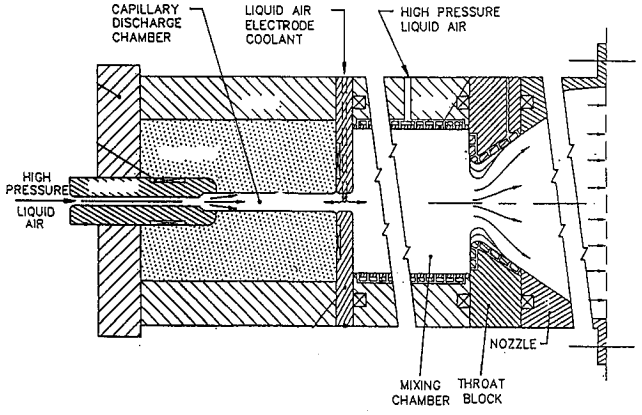

Fig. 2 Schematic of the electrothermal wind-tunnel concept.

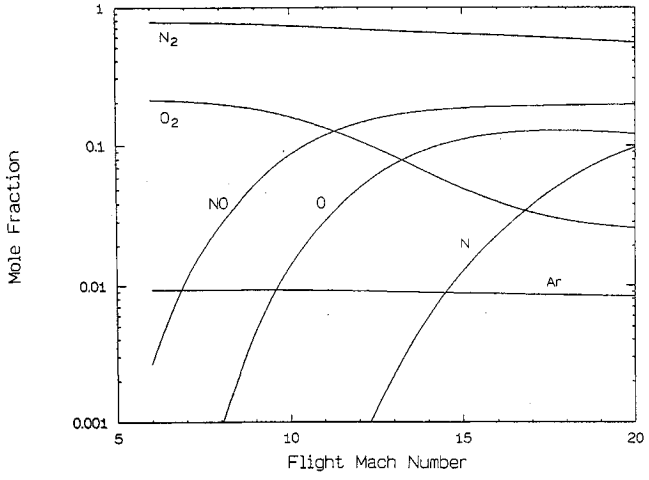

Fig. 3 Equilibrium composition of air at the reservoir conditions (major species).

conversion efficiency of between 50–60%. Finally, use of a liquid permits relatively large mass flows with physically compact chambers, pumping equipment, etc. Hence, the overall scale, and therefore cost of the facility, is significantly reduced while at the same time permitting higher pressures to be tolerated.

Gas Conditions in the Mixing Chamber (Reservoir)

The function of the mixing chamber (reservoir) of the EWT is to receive the arc-heated gases discharged from the capillary and dilute them with additional fluid to achieve the desired gas composition, pressure and enthalpy. Simulating Mach 10–20 scramjet test conditions in the EWT facility requires that the test gas be generated in the mixing chamber at true total enthalpy and pressure. At these flight conditions (especially above Mach 15), the test gas will be calorically imperfect, highly dissociated, and partially ionized in the mixing chamber. The net effect is that the chamber pressure will be higher and the temperature lower than those predicted assuming a perfect gas.

Mixing chamber conditions were calculated by isentropically stagnating the flow from the flight or local static conditions. Chemical equilibrium was assumed in the mixing chamber (this assumption was verified by finite rate calculations at several conditions) and was calculated with a high temperature chemistry code "EqState" which uses the CREK chemistry package developed by Pratt.[8]

The calculated reservoir conditions and principal species are shown in Fig. 3. At Mach 10, the mixing chamber composition shows increasing levels of nitric oxide formation, but trace concentrations of atomic oxygen and nitrogen. At Mach

16 to 20, significant amounts of atomic oxygen form due to dissociation despite the high total pressures. In addition, nitric oxide and other species begin to ionize. Similar calculations were made for inlet and combustor entrance conditions which showed an increase in dissociation of molecular species due to lower total pressures.

Compressibility Effects

In addition to the caloric imperfection and dissociation of air at high total enthalpies, the density in the mixing chamber at these conditions is such that the ideal gas equation of state becomes invalid. The equation was corrected for compressibility effects by introducing the second and third virial coefficients calculated from the Lennard-Jones (6–12) and square-well potential functions. The methods in Refs. 9 and 10 were used to estimate the force constants for gas mixtures.

The mixture compressibility factor (due only to intermolecular forces, i.e., thermal imperfection) in the reservoir was calculated for each facility design point listed in the Appendix. The results show a significant increase in the reservoir gas compressibility with flight Mach number for free-jet simulation. At Mach 16, for example, the required free-jet pressure is 50% higher than the calculated pressure in Fig. 1, or about 13,000 atm. Since the total pressure varies exponentially with Mach number, the reduction in Mach number simulation is not substantial. In this case, if 13,000 atm is considered the maximum containable pressure, then full free-jet simulation is reduced from Mach 17 to 16. At Mach 20, the compressibility factor (2.8) raises the required reservoir pressure to 112,000 atm from 40,000 atm. Clearly, these effects must be included in any estimation of required reservoir pressures at Mach numbers above 10.

The implications of gas compressibility on facility nozzle performance are, to first order, minimal if the predicted real gas reservoir pressure can be contained. In effect, at the real gas pressure, the temperature-density history (and hence, the chemistry) through the nozzle would be similar to that for an ideal gas (neglecting the second-order effect of the change in reservoir pressure on the mixture composition). If, however, the real gas total pressure cannot be contained, then the effect would be to reduce the initial density accordingly, resulting in poorer nozzle chemical kinetic performance. The chemical kinetic nozzle calculations made during this study did not incorporate compressibility effects, so that the results may be assumed similar to those in which compressibility effects were included and the total pressure was increased according to the real gas calculations described.

Chemical Kinetic Nozzle Performance

Expansion of the gas through a facility nozzle to achieve the desired test conditions requires proper consideration of the coupled chemical and gas dynamic processes, the goal being to assure a test flow which is as consistent as possible with that encountered in flight where low concentrations of nitric oxide and atomic oxygen are expected in the airstream entering a scramjet combustor even at near-orbital speeds. This is due to the low temperature prevailing through most of the inlet, and the very short residence time in the last segment of the inlet where the temperatures are high. However, both nitric oxide and atomic oxygen are capable of dramatically altering autoignition characteristics at low temperatures and/or pressures where ignition delay times are significant.[11] The overall heats of combustion of hydrogen, for example, with nitric oxide or with atomic oxygen are considerably higher (36 and 100%, respectively) than with molecular oxygen. Accordingly, reduction of these species to tolerable levels in the test gas is considered essential, and was the focus of the calculations made here.

The one-dimensional finite rate calculations were made with the LSENS general chemical kinetics code, which is a revision of the GCKP84 code written by Bittker and Scullin.[12] The code was modified to accept high temperature (>5000 K) polynomial curve fits for the thermodynamic properties of the constituents of air, including ionized species. The neutral species chemical kinetic mechanism used for the calculations was compiled by Ref. 13 and the ion reaction mechanism was obtained from Bortner.[14]

Initial conditions were taken at the nozzle throat where the gas was calculated to be in chemical equilibrium after an adiabatic expansion to the sonic state. Of course, the actual nozzle will be cooled and significant wall heat transfer may occur in this region. However, without knowledge of the cooling mechanism and the resulting heat transfer rate, and given the other assumptions implicit in this type of calculation, assuming an adiabatic flow suffices.

All of the calculations in this section assume that the flow is vibrationally equilibrated with the translational mode. The high pressures which prevail through the nozzles for these conditions, combined with the relatively low expansion angles examined, will almost certainly produce a flow which is vibrationally equilibrated. In addition, the effect of ion reactions on the chemistry was found to be negligible due to the small fraction of total enthalpy (0.5%) consumed by the ions in the flow.

Expansion Angle Variation

Calculations were made to determine the extent of oxygen recombination for a range of conical nozzle half-angles from 2 to 10 deg. The low nozzle half-angles investigated here are not representative of realistic or typical values, but were used to study finite rate chemistry nozzle performance over a relatively wide range of expansion rates. Expansion rates as low as 2 deg would most likely introduce excessive boundary-layer growth and would exacerbate the heat transfer problem near the throat. On the other hand, at flight conditions above about Mach 14, the degree of recombination chemistry is more heavily dependent on the expansion angle, so that consideration must be given to lower initial angles than are typically used for current facility nozzles.

In all of the nozzle geometries and conditions examined, most of the recombination was seen to occur very early in the expansion. This is typical of all the nozzles examined in this study (and facility nozzles in general). In addition, the concentration histories for a particular reservoir condition are independent of the expansion rate within the given range of nozzle half-angles. This implies that the chemistry is initially in equilibrium with the local thermodynamic conditions due to the high local densities. At sufficiently low densities, however, chemical equilibrium cannot be maintained, and the freezing rate then becomes a function of the rate of change of the local conditions.

Mach 10 and 12 Nozzles

The solutions for the Mach 10 and 12 conditions are summarized in Fig. 4. Shown are the nozzle exit mole fractions of nitric oxide and molecular oxygen vs the nozzle half-angle. Note that the test gas mixture is relatively independent of expansion angle at these conditions. Also, although no atomic oxygen remains after expansion to the test condition, nitric oxide freezes at relatively high levels (about 5% by volume). Since nitric oxide is a stable compound and its formation is enhanced by high pressure, it is unlikely that reductions in its concentration can be made without significantly altering the composition of the mixture. However, calculations were made which indicate that the oxygen lost to nitric oxide can be replaced without additional formation of atomic oxygen or NO.

Mach 16 Nozzle

The results for the Mach 16 nozzle shown in Fig. 5 indicate that atomic oxygen remains in the test gas in the free-jet nozzle (1–3%), but to a much greater extent in the direct connect

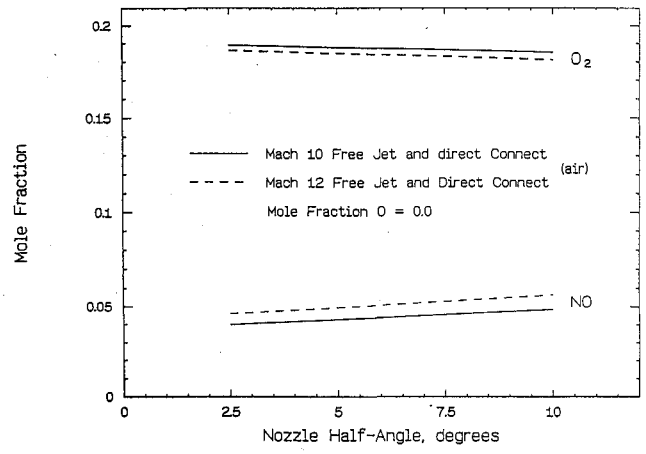

Fig. 4 Calculated oxygen and nitric oxide concentrations at the facility nozzle exit vs expansion angle (Mach 10 and 12 conditions).

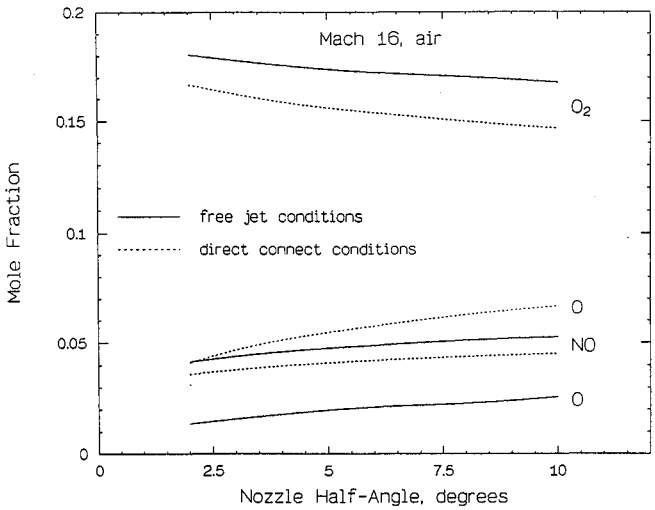

Fig. 5 Calculated atomic and molecular oxygen and nitric oxide concentrations at the facility nozzle exit vs expansion angle (Mach 16 conditions).

nozzle (4–7%). In addition, the dependence of the composition on the expansion angle increases. However, the concentration of nitric oxide freezes at about the same level (4–5%) as for the Mach 10 and 12 nozzles. This is in fact seen to be the case at all the conditions examined here. Since the predicted gas composition after expansion may be marginally acceptable for combustion testing, this flight condition was the focus of subsequent calculations.

Oxygen replenishment was evaluated as a method for increasing the concentration of molecular oxygen in the test gas without additional formation of unwanted species. The methodology was simply to increase the undissociated concentration of oxygen, and observe the nozzle exit concentrations predicted by the finite rate solution until a 21% mole fraction of oxygen was obtained. These calculations indicate that make-up oxygen can be added with an insignificant increase in dissociation products in the test gas.

In an attempt to reduce the atomic oxygen concentration in the test gas, a small amount of water (5% by volume) was added to act as a three-body recombination catalyst. Although there are many other such catalysts available (e.g., metal oxides), their principal disadvantage is that they contaminate the flow with unwanted elements that may have a significant effect on the chemical processes occurring in the combustion zone. In addition, condensation near the nozzle exit may disturb the core flow and threaten the model and its instrumentation.

It was found that the initially dissociated water tended to almost completely recombine and that the atomic oxygen concentration was reduced to trace amounts (1.7×10^{-4}). However, trace concentrations of hydroxyl radicals and other hydrogen-air combustion intermediates also remain at the exit which may have a significant effect on ignition delay times at conditions near the autoignition limit of hydrogen (1000 K). However, since combustor entrance temperatures at Mach 16 are close to 2000 K, it is unlikely that trace concentrations of OH will alter the combustion process. Hence, the results are encouraging in that there is a significant reduction in the concentration of atomic oxygen due to the introduction of water.

Mach 20 Nozzle

For Mach 20 simulation, the nozzle exit compositions shown in Fig. 6 consist mostly of atomic oxygen and vary substantially with the expansion angle. Obviously, the chemical composition of the gas after expansion to a Mach 20 test condition will not be suitable for combustion simulation.

Correlation of Recombined Oxygen with Reservoir State and Nozzle Geometry

It has been observed[15,16] that the chemical state of the gas for which freezing occurs after a nonequilibrium expansion correlates with the reservoir entropy. However, no such correlation was found. The implication is that within this reservoir entropy range the nonequilibrium processes which determine the final mixture composition may be sensitive to other characteristics of the expansion as well.

By considering the entropy change due to changes in mixture composition, a correlation was found between the oxygen which recombines in the nozzle and the reservoir entropy, pressure, enthalpy, and the nozzle half-angle. This "nozzle performance" parameter is

$$\eta_n = s_t \frac{[P_t(\text{atm})/\tan\theta]}{H_t}, \qquad (K^{-1})$$

The form of this parameter is appropriate since higher total temperatures (enthalpies) tend to reduce recombination rates, making chemical performance inversely proportional to the total enthalpy. In contrast, higher total pressures delay chemical freezing, and therefore, will increase nozzle performance. The expansion angle changes the effective total pressure, with larger angles promoting freezing of the composition. η_n is

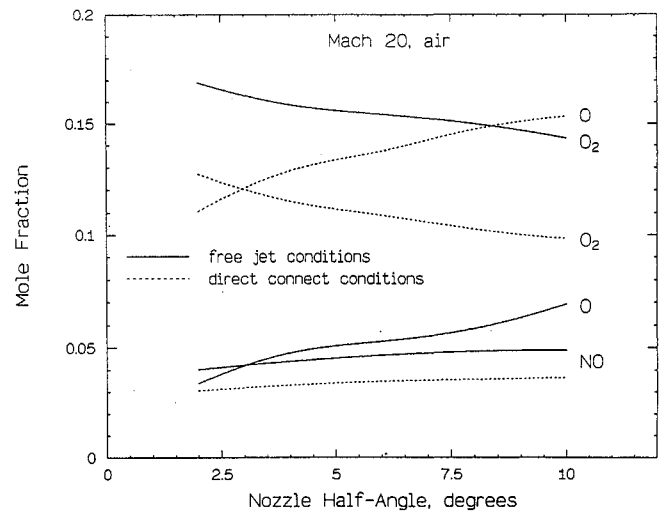

Fig. 6 Calculated atomic and molecular oxygen and nitric oxide concentrations at the facility nozzle exit vs expansion angle (Mach 20 conditions).

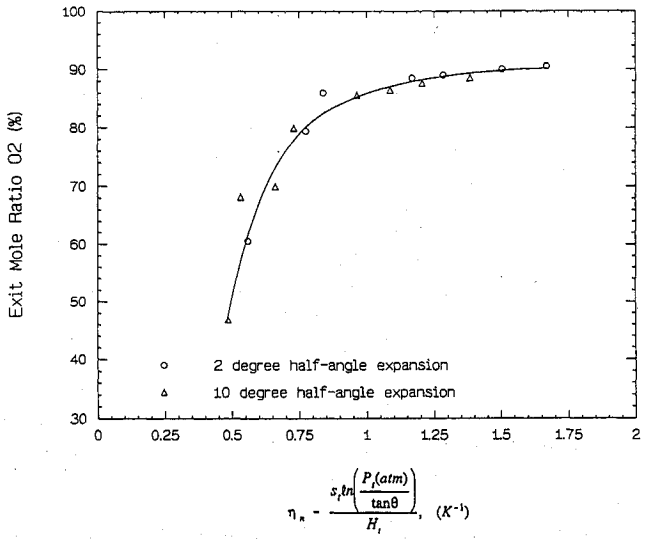

Fig. 7 Correlation of nozzle exit mole ratios of oxygen with the nozzle performance parameter.

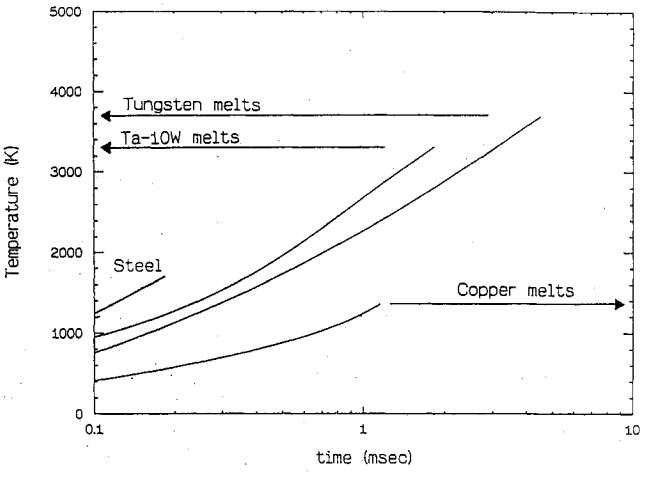

Fig. 8 Wall temperature time histories for various heat sink materials.

plotted in Fig. 7 as a function of the ratio of nozzle exit mole fraction of oxygen to the nominal mole fraction (0.21) in percent, for all the conditions examined and for expansion half-angles of 2 and 10 deg. The points asymptote to slightly above 90% recombination of oxygen. The deficit is in the nitric oxide. The implication here, as observed above, is that nitric oxide is always formed somewhere in the reservoir at the conditions considered and, once formed, the oxygen lost to nitric oxide cannot be recovered. Values of η_n below about 0.0075 result in a substantial drop in the amount of oxygen recombined. Extrapolating the curve to 0% recombined oxygen results in a value of η_n of about 0.0025. A reflected shock tunnel operating at Mach 25 total enthalpy with about 350 atm of total pressure produces almost 100% dissociated oxygen in the test section. Assuming an effective expansion half-angle of 8 deg, η_n for this simulated condition is 0.0031. The agreement is good given the slope of the curve at this value of η_n.

Facility Nozzle Throat Heat Transfer

The previous discussion of reservoir conditions makes clear that the mixing chamber and the facility nozzle throat will encounter high temperatures and pressures. In addition, the test times contemplated for this facility are sufficiently long that significant heat conduction will occur through the nozzle walls. A preliminary assessment was made of the transient temperature and heat flux distribution at the throat for the facility design points. Various heat dissipation methods were then investigated, including heat sinks, ablative inserts, and transpiration cooling.

Temperature Response for a Heat Sink Throat

The transient temperature response of a heat sink throat was modeled by assuming a one-dimensional convection boundary condition for a semi-infinite solid. The convective heat transfer coefficient was estimated from an empirical Nusselt number correlation for turbulent, fully developed flow in smooth pipes. The resulting temporal surface temperatures are shown in Fig. 8 for throat conditions corresponding to Mach 16 direct connect simulation, and for heat sink throats composed of OFHC copper, 1020 carbon steel, pure tungsten, and a 90% tantalum—10% tungsten alloy (Ta-10W). It is clear that no heat sink material will survive more than a few milliseconds at this condition, and that the refractory metals are not much better than copper in surviving this environment. In fact, copper alloys having higher melting points than pure copper, but retaining a high thermal conductivity, e.g., "Narloy Z" (Cu-0.1Z), may outlast the refractory metals.

These wall temperatures suggest that for a test time of 0.2 s an uncooled throat may suffice at Mach 10–12. Above Mach 12, the surface temperature over this test time rises to almost the freestream value. At Mach 16, the average heat flux over the test time is significantly greater than typical heat fluxes encountered in rocket nozzle throats, which are between 2–5 kW/cm^2, and about one order of magnitude greater than the stagnation point heat flux of a ballistic missile during reentry at low altitude. The heating rates at Mach 20 conditions seem well beyond current technology.

Table 1 Area changes

Test time, s	Percent area change
0.1	6.7
0.2	13.6

Ablative Throat Inserts

Preliminary estimates were made of the possibility of using an easily replaceable throat insert (liner) and permitting some ablation during each test. The philosophy is, if the throat area increase during the test time is sufficiently small (i.e., so that the facility nozzle exit Mach number change is similar to Mach number changes along a flight path in a similar time frame), then ablation may represent the most cost-effective method of dealing with the high throat heat fluxes.

To this end, the methods developed in Ref. 17 were used. The problem treated therein is the re-entry stagnation point heat transfer problem, which is clearly a different situation than encountered here. On the other hand, the lack of data at these extreme conditions ("sublimation" temperatures, latent heats, etc.) required the use of "normal" values for these quantities, driving the results in directions that must be subsequently assessed. Tungsten was assumed to be the throat insert material. Pure tungsten may not be the material ultimately selected, but was used by way of illustration because its properties are well known. Area changes were determined for a Mach 16 direct connect nozzle (Table 1).

Of consequence is the fact that the area changes cited suggest that an ablative wall may be an acceptable approach to dealing with the throat problem. However, the flow development of a high Mach number nozzle is particularly sensitive to disturbances (mass transfer, oxidation, surface roughness, etc.) in the boundary layer near the sonic region. The effects of these disturbances on the nozzle core flow must be assessed.

Transpiration-Cooled Throat

Estimates of the coolant mass flow required for a given reduction in heat transfer coefficient were determined from semi-empirical correlations based on a mixing length theory for coolant gases injected into air.[18,19] The blowing factor, or the required coolant to total mass flow ratio, was calculated from this correlation for a Mach 16 direct connect nozzle throat. The coolant (helium) and porous structure (tungsten) were assumed to be in equilibrium at a surface temperature of 2000 K. The heat transfer coefficient required to maintain this surface temperature is 13.3 kW/m^2-K giving a reduction in heat transfer coefficient of 0.053. The corresponding blowing factor of 0.0036 is large compared to typical values of 0.0002.

There are several other problem areas which must be addressed before transpiration cooling is determined to be a practical solution. First, the structural material must be formed such that the pores possess small hydraulic diameters on the order less than 0.001 in. Significantly larger pores result in a decrease in cooling efficiency which approaches that of film cooling. If the porous material has a three-dimensional flow characteristic, then the distribution of coolant mass flow will be dependent on the pressure drop through the material, and local hot spots may develop on the surface. Secondly, the effect of the transpired coolant on the stability and development of the boundary layer and the expanding core flow must be determined, with the obvious objective being to minimize disturbance to the core flow. Resolution of these issues will require sophisticated CFD in concert with experimental verification.

Power Requirements for the EWT

The power requirement for an electrothermal wind tunnel operating for 0.5 s at Mach 20 total enthalpy with a mass flow of 17 kg/s (37 lb/s) was assessed. Operating on a pulsed basis, the flat-top of the pulse is assumed to be 0.5-s long, with a ramp-up of a few tenths of a second, and a rapid shut-down of a tenth second or less. The startup and shutdown increase the total energy requirement from current zero to current zero by about 50%. Assuming that the electrothermal heater is 55% efficient, the total electric power and energy requirements are 650 MW and 500 MJ, respectively. If Mach 16 is assumed to be the simulation limit, then the required power and energy are reduced to 400 MW and 300 MJ.

Preliminary Simulation Envelope

The simulation envelope of the EWT was estimated based on the above considerations. That is, the range of flight conditions which would result in acceptable nozzle performance, containable total pressures, throat heat flux considerations, and power supply limits. The results of these calculations are shown in Fig. 9, which maps the portions of the flight envelope where these conditions are met. The solid lines represent flight paths for flight dynamic pressures of 500–2000 psf. The dashed and dotted lines bound the simulation regime for the direct connect and free-jet conditions, respectively. Simulation of free-jet conditions is seen to be limited by the total pressure and throat heat flux generated. Direct connect simulation is limited by nozzle kinetic performance to Mach 16 at q = 1000 psf and to about Mach 13 at q = 2000 psf. The remainder of the flight envelope is bounded by power limitations.

Experimental Study

The objective of the experimental work was to demonstrate stable operation of the capillary arc with a cryogenic liquid as the working fluid. To this end, a subscale EWT was designed, built, and tested. The wind tunnel, shown schematically in Fig. 10, consists of basically three components: 1) an

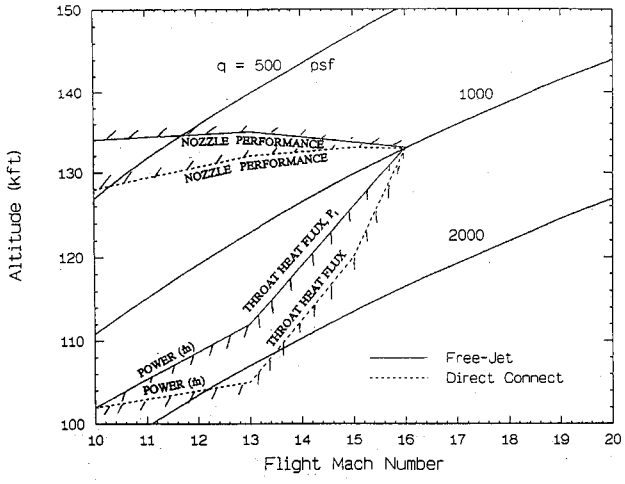

Fig. 9 Preliminary EWT simulation envelope.

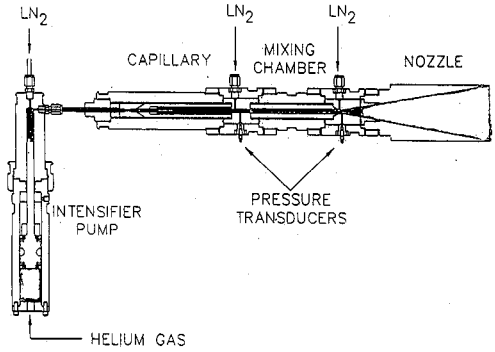

Fig. 10 Schematic of the experimental, subscale EWT.

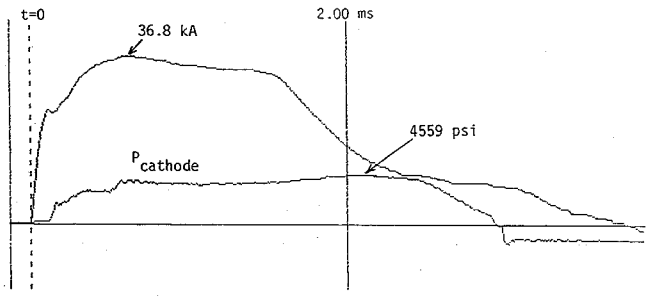

Fig. 11 Liquid nitrogen test: measured current and capillary exit pressure.

arc discharge chamber (capillary), 2) a cryogenic pump to feed liquid to the capillary, and 3) a nozzle to receive and expand the vapor effluent. The capacitive pulse-forming network (PFN) supplied constant current for 2 ms to the capillary. Peak power during the pulse was nominally 40 MW delivered by 20 kA at 2.0 kV.

Liquid nitrogen (LN_2) was introduced into the capillary by way of the intensifier pump. A stable arc was established in two tests. Figures 11 and 12 show the temporal capillary and nozzle throat pressure traces, respectively, with the current superimposed on each trace for reference. Steady current is maintained for approximately 1 ms as the transients consume about one-half of the total energy. Initial peaks and subsequent oscillations in the traces result from variations in the vaporization rate of the LN_2 which changes the path resistance through the capillary. The capillary pressure rises to a peak value of about 4600 psi (Fig. 12) and remains steady for about 1.5 ms. The nozzle throat pressure rises to about 2200 psi,

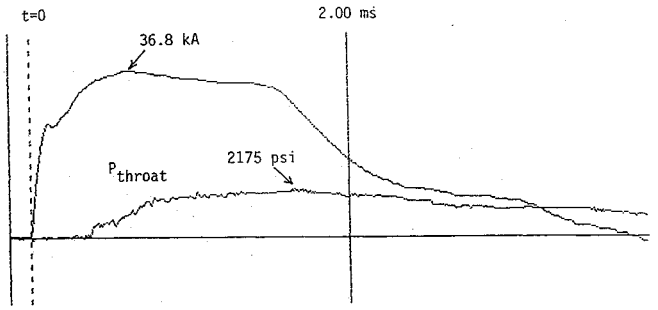

Fig. 12 Liquid nitrogen test: measured current and nozzle throat pressure.

indicating that the total pressure loss through the mixing chamber is small.

Because of problems with the cryogenic pump, the pump pressure was below the peak stagnation pressure in the capillary on the last two tests. Hence, the mass flow rate dropped to zero relatively early in the discharge. However, the lack of any deleterious effects on the arc discharge during the current rise time when $P_{pump} > P_{capillary}$ is strong evidence that the arc would have survived a higher injection pressure during the peak current part of the discharge. Establishment of a stable arc discharge appears to be relatively straightforward, as suggested by the two test shots discussed here.

Conclusions

The analytical and experimental results of a study to assess the feasibility of building a Mach 10 to 20, high-pressure electrothermal wind tunnel were presented. The analytical study was performed to determine the practical simulation limits of the facility. The conclusion was that the facility is capable of simulation conditions suitable for hypervelocity air breathing propulsion testing up to Mach 16, where pressure containment, high nozzle throat heat flux rates, and chemical freezing in the nozzle become limiting factors. In addition, the high total pressure capability improves the recombination chemistry in the facility nozzle by allowing chemical equilibrium to prevail to the freezing point. However, the high pressure also enhances the formation of nitric oxide which contaminates the test gas at roughly 5% by volume throughout the simulation envelope. The oxygen lost to nitric oxide can be replenished in the reservoir with no additional chemical freezing of dissociation products. Atomic oxygen begins to freeze out at about Mach 15 simulated conditions, but can be significantly reduced by using water to effectively catalyze the three-body recombination reactions. Finally, a nozzle performance parameter was identified which correlates the amount of recombined oxygen in the nozzle to the reservoir conditions and the nozzle expansion rate for the test conditions examined.

The experimental study was conducted to determine the operational characteristics of the electrothermal heater with liquid air as the working fluid. The tests indicated that a steady arc discharge can be maintained with liquid nitrogen flowing through the arc chamber (capillary). Discharge data was limited, however, and full operating pressure (60,000 psi) (and hence, mass flow) was not obtained due to equipment problems with the cryogenic pump. However, the measured capillary pressure is still 20% greater than the maximum total pressure obtainable in conventional arc heaters.

Appendix: EWT Tunnel Conditions

Table A1 shows the inlet conditions behind the shock of an 8-deg forebody. Table A2 shows the combustor entrance conditions after compression by a "low contraction ratio" adiabatic inlet.[20] Flight dynamic pressure = 1000 psf.

Table A1 Free-jet

M_∞	H_l, MJ/kg	P_l, kN/m^2	T_l, K	V_l, m/s	M_l	$\dot{m}$, kg/s[a]
10	4.7	3.6	420	3000	7.3	17
12	7.2	3.2	490	3660	8.3	15
16	13	2.8	670	5010	9.8	13
20	21	2.6	870	6380	11	12

[a]For 2-ft^2 test area.

Table A2 Direct-connect

M_∞	P_l, kN/m^2	T_l, K	V_l, m/s	M_l	$\dot{m}$, kg/s[a]
10	63	1300	2660	3.8	17
12	61	1500	3350	4.5	15
16	56	2100	4700	5.4	13
20	53	2700	5960	5.9	12

[a]For 2-ft^2 test area.

Acknowledgments

The work presented in this article was conducted under NASA Contract NAS1-18450. The NASA program monitors were Ernest Mackley, Dennis Bushnell, and Griffin Anderson. The authors are pleased to acknowledge their guidance, cooperation, and assistance in carrying out this effort. The authors also wish to acknowledge John Erdos for his contributions and for the benefit of many useful discussions regarding the work carried out under this contract.

References

[1]Roffe, G., "Hypersonic Scramjet Test Facility Concept Study," General Applied Science Labs. TR 295, June 1988.

[2]Thomas, S. R., and Guy, W., "Scramjet Testing from Mach 4 to 20, Present Capabilities and Needs for the Nineties," AIAA Paper 90-1388, June 1990.

[3]Wagner, D. A., Varner, M. O., Williams, R. R., and Griffith, B. J., "Hypersonic Facility Requirements and Design Considerations," AIAA Paper 88-1991, May 1988.

[4]Wagner, D. A., Smith, R. K., and Gunn, J. A., "Hypersonic Test Facility Requirements for the 1990's," AIAA Paper 90-1389, June 1990.

[5]Anderson, G. Y., "An Outlook on Hypersonic Flight," AIAA Paper 87-2074, June–July 1987.

[6]Winsor, N. K., Massey, D., Goldstein, S. A., Tidman, D. A., Greig, J. R., Napier, P. A., Hilko, B. K., and Burton, R. L., "Facility Description: A 20 mm Electrothermal Gun," GT-Devices, 38th Meeting, Aeroballistic Range Association, Tokyo, Japan, Oct. 1987.

[7]Burton, R. L., Fleischer, D., Goldstein, S. A., and Tidman, D. A., "Experiments on a Repetitively Pulsed Electrothermal Thruster," *Journal of Propulsion and Power*, Vol. 6, No. 2, 1990, pp. 139–144.

[8]Pratt, D. T., "Calculation of Chemically Reacting Flows with Complex Chemistry," *Studies in Convection*, edited by B. E. Lauder, Vol. 2, Academic Press, New York, 1977.

[9]McBride, B. J., Heimel, S., Ehlers, J. G., and Gordon, S., "Thermodynamic Properties to 6000 K for 210 Substances Involving the First 18 Elements," NASA SP-3001, 1963.

[10]Reid, R. C., and Leland, T. W., Jr., "Pseudocritical Constants," *A.I.Ch.E. Journal*, March 1965, pp. 228–237.

[11]Rogers, R. C., and Schexnayder, C. J., Jr., "Chemical Kinetic Analysis of Hydrogen-Air Ignition and Reaction Times," NASA TP 1856, July 1981.

[12]Bittker, D. A., and Scullin, V. J., "GGKP84—General Chemical Kinetics Code for Gas-Phase Flow and Batch Processes Including Heat Transfer Effects," NASA TP 2320, Sept. 1984.

[13]Oldenborg, R., Chinitz, W., Friedman, M., Jaffe, R., Jachimowski, C., Rabinowitz, M., and Schott, G., "Status Report of the Rate Constant Committee, NASP High Speed Propulsion Technology Team," Dec. 1989.

[14]Bortner, M. H., "Reaction Rate Handbook," DASA 1948, General Electric Co., Philadelphia, PA, Chap. 19, Oct. 1967.

[15]Harris, C. J., "Comment of Nonequilibrium Effects on High-

Enthalpy Expansion of Air," *AIAA Journal*, Vol. 4, No. 6, 1966, pp. 1148, 1149.

[16]Lordi, J. A., and Mates, R. E., "Nonequilibrium Effects on High-Enthalpy Expansions of Air," *AIAA Journal*, Vol. 3, No. 10, 1965, pp. 1972–1974.

[17]Truitt, R. W., *Fundamentals of Aerodynamic Heating*, Ronald Press, New York, 1960, Chap. 11.

[18]Rohsenhow, W. M., and Hartnett, J. P., *Handbook of Heat Transfer*, McGraw-Hill, New York, 1973, pp. 19–32.

[19]Schlichting, H., *Boundary Layer Theory*, McGraw-Hill, New York, 1979.

[20]Billig, F. S., Waltrup, P. J., Gilreath, H. E., White, M. E., Van Wie, D. M., and Pandolfini, P. P., "Proposed Supplement to Propulsion System Management Support Plan," Unclassified, Controlled Need to Know, The Johns Hopkins Univ./Applied Physics Lab. NASP-88-1, Laurel, MD, July 1986.

Modern Engineering for Design of Liquid-Propellant Rocket Engines

Dieter K. Huzel and David H. Huang

From the component design, to the subsystem design, to the engine systems design, engine development and flight-vehicle application, this "how-to" text bridges the gap between basic physical and design principles and actual rocket-engine design as it's done in industry. A "must-read" for advanced students and engineers active in all phases of engine systems design, development, and application, in industry and government agencies.

Chapters: Introduction to Liquid-Propellant Rocket Engines, Engine Requirements and Preliminary Design Analyses, Introduction to Sample Calculations, Design of Thrust Chambers and Other Combustion Devices, Design of Gas-Pressurized Propellant Feed Systems, Design of Turbopump Propellant Feed Systems, Design of Rocket-Engine Control and Condition-Monitoring Systems, Design of Propellant Tanks, Design of Interconnecting Components and Mounts, Engine Systems Design Integration, Design of Liquid-Propellant Space Engines PLUS: Weight Considerations, Reliability Considerations, Rocket Engine Materials Appendices, 420 illustrations, 54 tables, list of acronyms and detailed subject index.

AIAA Progress in Astronautics and Aeronautics Series
1992, 431 pp, illus ISBN 1-56347-013-6
AIAA Members $89.95 Nonmembers $109.95 Order #: V-147

Place your order today! Call 1-800/682-AIAA

AIAA
American Institute of Aeronautics and Astronautics

Publications Customer Service, 9 Jay Gould Ct., P.O. Box 753, Waldorf, MD 20604
FAX 301/843-0159 Phone 1-800/682-2422 9 a.m. - 5 p.m. Eastern

Sales Tax: CA residents, 8.25%; DC, 6%. For shipping and handling add $4.75 for 1-4 books (call for rates for higher quantities). Orders under $100.00 must be prepaid. Foreign orders must be prepaid and include a $20.00 postal surcharge. Please allow 4 weeks for delivery. Prices are subject to change without notice. Returns will be accepted within 30 days. Non-U.S. residents are responsible for payment of any taxes required by their government.